The three-dimensional structure of an upper ocean vortex in the tropical Pacific Ocean

Pierre J. Flament*, Sean C. Kennan*, Robert A. Knox†, Pearn P. Niiler†, and Robert L. Bernstein‡

* School of Ocean and Earth Science and Technology, University of Hawaii, Honolulu, 1000 Pope Rd, Hawaii 96822 USA

† Scripps Institution of Oceanography, University of California San Diego, San Diego, La Jolla, California 92093-0230, USA

‡ SeaSpace, Inc., 9240 Trade Place suite 100, San Diego, California 92126, USA

Reprinted from Nature, Vol 383, No 6601, 17 october 1996.

In the equatorial Pacific Ocean, easterly trade winds and the Earth's rotation combine to drive surface currents away from the Equator, thereby causing cold nutrient-rich subsurface water to upwell. The front [1] that forms between this upwelled water and warmer waters north of the Equator is sometimes visible as a spectacular "line in the sea" [2] between 2° and 6°N. Westward-propogating cusp-shaped disturbances observed along this front [3] have been attributed to the effect of dynamical instabilities in the system of zonal equatorial currents [4, 5, 6, 7, 8, 9, 10, 11] but the connection between these phenomena remains unclear. Here we report extensive measurements from shipboard sensors, satellite and drifting buoys which reveal the three-dimensional structure of an anticyclonic eddy (or vortex) ∼500-km in diameter and centred at 4°N. We suggest that the cusp-shaped disturbances at the front are caused by trains of large-amplitude vortices, which are driven by instability of the mean zonal shear. We show that these vortices not only play an important role in the meridional transport of heat, salt and momentum, but are also associated with regions of intense horizontal convergence along the front, where dramatic concentrations of marine life are observed.

The sheared zonal equatorial currents system (ECS), consisting of the westward south equatorial current (SEC) at 2°S-3°N, the eastward equatorial undercurrent (EUC), and the eastward north equatorial counter current (NECC) at 5°N-10°N, is subject to westward propagating perturbations at periods of 15 to 30 days, first observed as meanders of the Atlantic equatorial currents [4]. They were subsequently identified in satellite images of sea surface temperature (SST) [3], drifting buoy trajectories [5], sea level and dynamic topography [12, 13], shipboard acoustic doppler current profiler (ADCP) sections [6], equatorial moored current meters time series [7, 8], and numerical model simulations [9, 10, 11]. The amplitude of these perturbations is largest when the ECS strengthens seasonally in boreal summer and autumn. They result presumably from dynamical instability of the ECS, although conversion of mean to eddy energy appears to occur at several latitudes, varying through the annual cycle [14, 15].

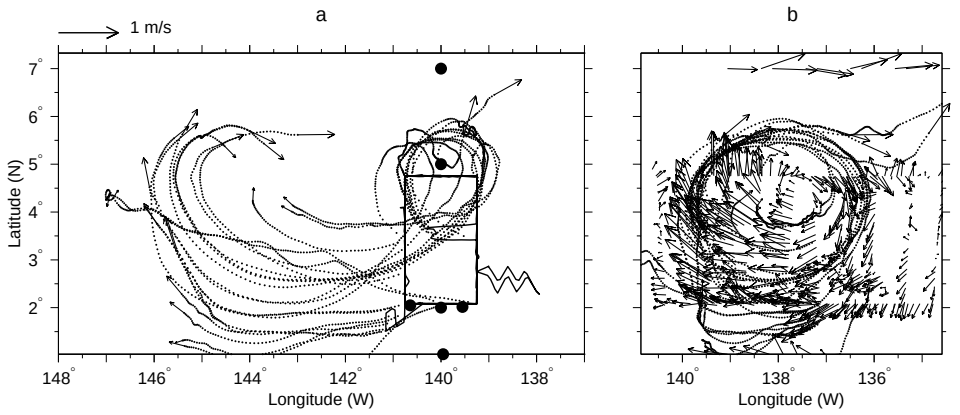

Figure 1: (a) Trajectories of the buoys between 17 November and 5 December 1990, dotted every 6 h. The last points are marked by velocity arrows. The track of the ship is shown by a solid line, and the positions of the moorings by filled circles. (b) Trajectories of the buoys in a frame of reference translating westward at 30 cm/s, with velocity vectors from ADCP and moorings superimposed (the longitude scale corresponds to the position of the vortex on 16 November 1990 00:00 UTC).

Repeated hydrographic surveys centred at 140°W 3°25'N were conducted in November 1990, with the objective of understanding the off-equatorial dynamics of these perturbations. The thermohaline fields were sampled with conductivity-temperature-depth (CTD) stations to 300 m depth spaced at 40 km, and near the fronts with CTD sensors attached to a towed platform (SeaSoar), undulating over 4 km [16]. A 150-kHz ship-mounted ADCP yielded profiles of velocity and backscatter intensity to 300 m depth; absolute velocities were computed using global-positioning system (GPS) navigation and the ship's gyrocompass. Forty satellite-tracked (ARGOS) buoys [17] drogued at 15 m depth were also deployed. Meteorological sensors were mounted on a bow tower to estimate the air-sea fluxes of heat, moisture and momentum by bulk-formulae [18, 19]. Additional measurements of wind, current and temperatures were obtained from moorings deployed by others (Eriksen, McPhaden [20], Weisberg [21]).

The drifting buoys followed typical cycloidal trajectories, often observed in this region [22], with a meridional amplitude of ∼400 km, a zonal wavelength of ∼600 km, and an orbital period of 20 days (Fig. 1a). Cycloids result from the superposition of a rotation and a translation; the translation speed inferred from the trajectories is 30 cm/s westward. Viewed in coordinates moving at this speed, velocity measurements from ADCP and moorings line up remarkably well with the buoy trajectories (Fig. 1b), despite their wide spatio-temporal separation in fixed coordinates. This indicates that the flow was approximately steady in the translating coordinates. The velocity, temperature, and salinity fields were therefore mapped in these coordinates, with a median interpolation of 70 km. The translation speed is robust: minimization of the interpolation error, fits to individual trajectories, and maximization of the correlation between longitude and

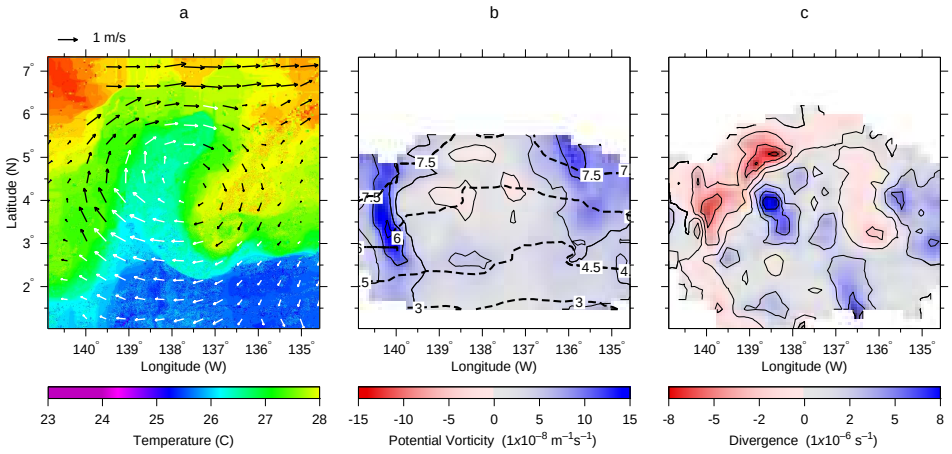

Figure 2: Fields in the moving frame of reference. (a) interpolated surface velocity; the background shows sea surface temperature from a satellite image on 16 November at 23:20 UTC, (b) total potential vorticity for the upper layer (the planetary component is contoured with dashed lines), (c) horizontal divergence at the surface.

meridional velocity, ADCP and mooring data included, yield the same speed, with a standard error of 1 cm/s.

The interpolated surface velocity (Fig. 2a) reveals a 500-km diameter anticyclonic vortex drifting along 4°24'N, straddled by the ∼0.60 m/s eastward NECC north of 6°30'N, and by the ∼0.75 m/s westward SEC south of 2°30'N. The zonal section through the centre (Fig. 3a) is asymmetric: the northward flow near 140°W peaked at 60 cm/s near the surface, while the southward flow near 137°W peaked at 75 m depth. The vortex was confined to the upper layer; below the 150-m deep thermocline, velocities were less than 10 cm/s. The density field was consistent with geostrophic balance, reflected by a deepening of the pycnocline in the core.

Remotely sensed SST (Fig. 2a) and zonal sections of temperature and salinity (Fig. 3b-c) show northward transport of equatorial water (relatively cold and saline from the upwelling), and southward transport of a shallow layer of warmer and fresher water (influenced by precipitation in the inter-tropical convergence zone, ITCZ). Cold and warm waters were separated by a sharp front, advected meridionally by the circulation of the vortex. The cusps generally seen in SST images [3] appear therefore to be the expression of such off-equatorial vortices, deforming the north equatorial front.

The spatial structure of the fields in the translating coordinates is equivalent to time series along a meridian. As about one period was sampled, the contribution of this vortex to meridional fluxes can be estimated by zonal averaging. At the surface, the heat flux (Fig. 4c) was southward and the salt flux (Fig. 4d) was northward everywhere, down the mean meridional gradients. The flux of zonal momentum (Fig. 4e) was negative south of 5°N, that is, there was a northward flux

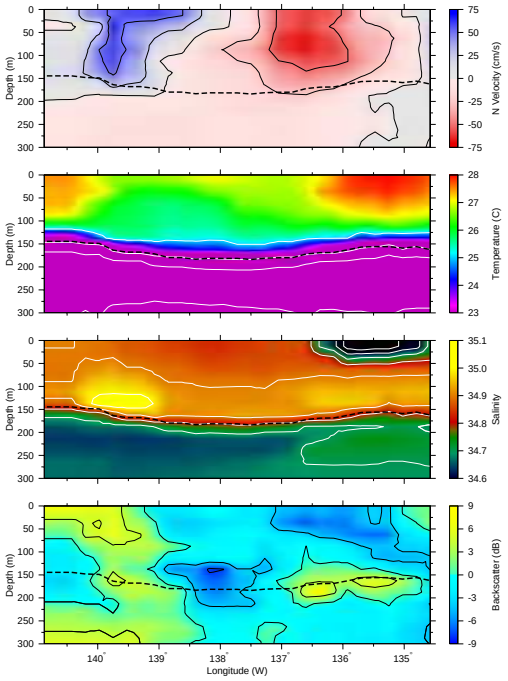

Figure 3: Zonal section through the vortex along 4°24′N: (a) meridional (northward) velocity component; (b) temperature, (c) salinity, (d) daytime acoustic backscatter at 150 kHz, normalized by the cruise-average profile. The 1024.5 kg m^{-3} isopycnal, conventionally chosen to identify the depth of the thermocline, is shown by a dashed line.

of westward SEC momentum; it diverged south of, and converged north of 3°40'N - about the latitude of the average position of the front. The large meridional momentum flux between 2°N and 5°N, acting to reduce the shear between the SEC and the NECC, suggests that the vortex was the finite amplitude result of an off-equatorial instability of the mean shear, in agreement with numerical model predictions [10, 11, 23].

During the ship surveys, the three moorings deployed along the Equator [21] recorded a meridional velocity oscillation of ∼70 cm/s amplitude and 18 d period. Cross-correlations of meridional velocity between adjacent equatorial moorings yielded an unambiguous westward propagation speed of 78 cm/s, in contrast with the 30 cm/s drift speed inferred for the off-equatorial vortex. This suggests that the vortex was distinct, and possibly decoupled, from the equatorial oscillations, known to be excited by shear within the SEC and between the SEC and EUC [14, 15, 21].

Convergence of the large scale wind-driven surface flow (the Ekman flow) [24] favours the formation of SST fronts. The curl of the zonally averaged wind stress (Fig. 4f) is negative

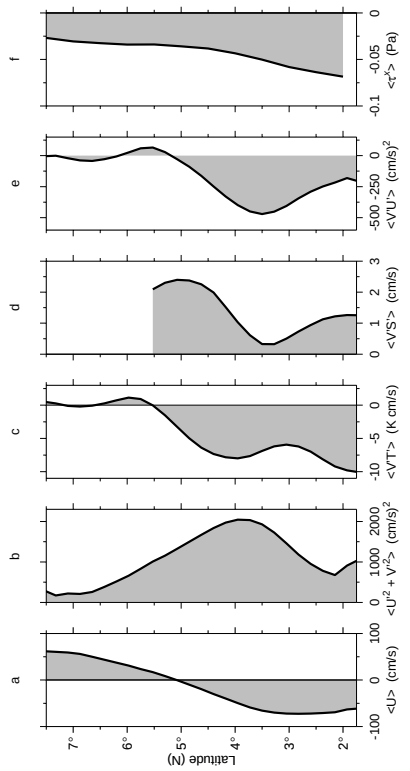

Figure 4: Zonally averaged quantities: (a), (b), mean zonal component of velocity ($< U >$;a) and eddy kinetic energy ($< U^2 + V^2 >$;b); (c), (d), (e), meridional fluxes of heat ($< V'T' >$;c), salt ($< V'S' >$;d) and zonal component of momentum ($< U'V' >$;e); (f), mean zonal wind stress ($< \tau^x >$.

between 2°30'N and 4°30'N, as southeasterly trade winds decrease towards the ITCZ. The Ekman flow is thus convergent, sharpening temperature and salinity gradients, and eventually leading to the formation of fronts. Similar Ekman fronts are observed in the North Pacific [25] and North Atlantic [26, 27] subtropical gyres.

Horizontal velocity gradients (that is, vorticity, divergence) offer further insight into the frontogenesis dynamics. The potential vorticity Q of a column of water, related to its angular momentum, is the ratio of the sum of planetary vorticity f (the vertical component of the Earth's rotation) and relative vorticity ζ (the rotation of the vortex with respect to the Earth), to the thickness H of the column: $Q = (f + \zeta)/H$. Potential vorticity of the upper layer (Fig. 2b) was conserved along streamlines, despite a twofold variation of planetary vorticity between 3°N and 6°N; relative vorticity was an important ingredient in this conservation. The near-zero

vorticity in the core suggests that the growth of the vortex may have been limited by inertial instabilities.

Vertical velocity, downwelling or upwelling, is directly related to horizontal velocity divergence (Fig. 2c). A long band of convergence, stretching from 140°W 3°30'N to 138°W 6°N, coincided with the leading edge of the front; it extended down the thermocline, implying vertical motions reaching 32 m/day. A similar pattern of convergence was predicted by numerical models [11]. The convergence band is consistent with the conservation of potential vorticity: as water columns move rapidly northward, their planetary vorticity f increases; to conserve potential vorticity Q, their thickness H must also increase (that is, the flow converges), further sharpening the Ekman front.

Convergence increases gradients of other advected properties such as zooplankton concentration, which can be estimated from the acoustic backscatter intensity of the ADCP [28]. A zonal section of backscatter anomaly (Fig. 3d), constructed using only daytime data to avoid bias due to the diurnal migration of zooplankton, shows an astounding increase of more than 20 dB above the background, aligned with the northward converging flow at 139°30 W. In the southward flow, the scattering layer was less intense and at the depth of the thermocline, suggesting that scatterers are subducted downwards while advecting around the vortex.

These new observations provide a synoptic synthesis of the causal links between large-scale atmospheric and oceanic flows, dynamical instabilities, finite amplitude vortices, frontogenetic processes, and eventual concentration of biological organisms. Intensification of the equatorial front in the presence of a vortex [29], increased density of phytoplankton [2, 30] and zooplankton [31] at the surface, and large accumulation of phytodetritus [32] at the sea bottom, were observed again during the 1992 Equatorial Pacific Joint Global Ocean Flux Experiment (JGOFS-EQPAC) [33], consistent with our findings from data collected in 1990.

Westward propagating perturbations of the ECS have been referred to as 'equatorial long waves' (Rossby gravity waves causing equatorial meanders of the EUC/SEC [8]), 'Legeckis Waves' (cusps in the north equatorial front, seen in satellite images [3]), and often, somewhat interchangeably, as 'tropical instability waves'. Our results, integrating data from a rich range of sensors, indicate that away from the Equator, they consist of finite amplitude vortices, drifting along the shear layer between the SEC and the NECC. Although when sampled from a fixed point, they appear as periodic oscillations of the fields, just as linear waves would, they are clearly trains of fully developed large-amplitude nonlinear eddies.

Moreover, within the limitations of the short sampling time, the observation of drastically different propagation speeds along the Equator and along 4.5N, suggests that the equatorial and subequatorial perturbations may at some times appear as distinct phenomena, contrary to general assumption. Whether this results from different forcing mechanisms, which may be phase-locked at some times of the year and decoupled at others (the vortex observed here was the last of the 1990 season), or from separate manifestations of the same instability, raises new questions concerning the dynamics of the equatorial current system in the Pacific.

References

[1] J. A. Knauss, "An observation of an oceanic front," *Tellus*, vol. IX, pp. 234–237, 1957.

[2] J. A. Yoder, S. G. Ackleson, R. T. Barber, P. Flament, and W. M. Balch, "A line in the sea," *Nature*, vol. 371, pp. 689–692, 1994.

[3] R. Legeckis, "Long waves in the eastern equatorial Pacific Ocean: A view from a geostationary satellite," *Science*, vol. 197, pp. 1179–1181, 1977.

[4] W. Düing, P. Hisard, E. Katz, J. Meincke, L. Miller, K. V. Moroshkin, G. Philander, A. A. Ribnikov, K. Voigt, and R. Weisberg, "Meanders and long waves in the Equatorial Atlantic," *Nature*, vol. 257, pp. 280–284, 1975.

[5] D. V. Hansen and C. A. Paul, "Genesis and effects of long waves in the equatorial Pacific," *J. Geophys. Res.*, vol. 89, pp. 10431–10440, 1984.

[6] D. Wilson and A. Leetmaa, "Acoustic Doppler Current Profiling in the equatorial Pacific in 1984," *J. Phys. Oceanogr.*, vol. 18, pp. 1641–1657, 1988.

[7] G. Philander, D. Halpern, D. Hansen, R. Legeckis, L. Miller, C. Paul, R. Watts, R. Weisberg, and M. Wimbush, "Long waves in the Equatorial Pacific Ocean," *EOS*, vol. 66, p. 154, 1985.

[8] D. Halpern, R. Knox, and D. Luther, "Observation of 20-day period meridional current oscillations in the upper ocean along the pacific equator," *J. Phys. Oceanogr.*, vol. 18, pp. 1514–1534, 1988.

[9] S. G. H. Philander, "Instabilities of zonal equatorial currents," *J. Geophys. Res.*, vol. 81, pp. 3725–3734, 1976.

[10] M. D. Cox, "Generation and propagation of 30-day waves in a numerical model of the Pacific," *J. Phys. Oceanogr.*, vol. 10, pp. 1168–1186, 1980.

[11] S. G. H. Philander, W. J. Hurlin, and R. C. Pacanowski, "Properties of long equatorial eaves in models of the seasonal cycle in the tropical Atlantic and Pacific Oceans," *J. Geophys. Res.*, vol. 91, pp. 14207–14211, 1986.

[12] C. Perigaud, "Sea level oscillations observed with Geosat along the two shear fronts of the Pacific North Equatorial Countercurrent," *J. Geophys. Res.*, vol. 95, pp. 7239–7248, 1990.

[13] L. Miller, D. R. Watts, and M. Wimbush, "Oscillations of dynamic topography in the eastern equatorial Pacific," *J. Phys. Oceanogr.*, vol. 15, pp. 1759–1770, 1985.

[14] D. S. Luther and E. S. Johnson, "Eddy energetics in the upper equatorial Pacific during Hawaii–to–Tahiti Shuttle Experiment," *J. Phys. Oceanogr.*, vol. 7, pp. 913–944, 1990.

[15] E. S. Johnson and D. S. Luther, "Mean zonal momentum balance in the upper and central equatorial Pacific Ocean," *J. Geophys. Res.*, vol. 99, pp. 7689–7705, 1994.

[16] R. T. Pollard, "Frontal surveys with a towed profiling conductivity/temperature/depth measurement package (seasoar)," *Nature*, vol. 323, pp. 433–435, 1986.

[17] P. P. Niiler, R. E. Davis, and H. J. White, "Water-following characteristics of a mixed-layer drifter," *Deep-Sea Res.*, vol. 34, pp. 1867–1882, 1987.

[18] S. Smith, "Coefficients for sea surface wind stress, heat flux and wind profile as a function of wind speed and temperature," *J. Geophys. Res.*, vol. 93, pp. 15467–15472, 1988.

[19] W. T. Liu, K. B. Katsaros, and J. A. Businger, "Bulk parameterization of air-sea exchanges of heat and water vapor including the molecular constraints at the interface," *J. Atmos. Sci*, vol. 36, pp. 1722–1735, 1979.

[20] M. J. McPhaden, "Monthly period oscillations in the Pacific North Equatorial Countercurrent," *J. Geophys. Res.*, vol. 101, pp. 6337–6359, 1996.

[21] L. Qiao and R. H. Weisberg, "Tropical instability wave kinematics: observations from the Tropical Instability Wave Experiment," *J. Geophys. Res.*, vol. 100, pp. 8677–8693, 1995.

[22] F. Chew and M. H. Bushnell, "The half-inertial flow in the eastern equatorial Pacific: a case study," *J. Phys. Oceanogr.*, vol. 20, pp. 1124–1133, 1990.

[23] K. A. Donohue, *Wave propagation in the central equatorial Pacific ocean*. PhD thesis, University of Rhode Island, 1995.

[24] J. Price, R. Weller, and R. Schudlich, "Wind-driven ocean currents and Ekman transport," *Science*, vol. 238, pp. 1534–1538, 1987.

[25] P. P. Niiler and R. Reynolds, "The three dimensional circulation near the eastern north pacific subtropical front," *J. Phys. Oceanogr.*, vol. 14, pp. 217–230, 1984.

[26] R. T. Pollard and L. Regier, "Large variations of potential vorticity at small spatial scales in the upper ocean," *Nature*, vol. 348, pp. 227–229, 1990.

[27] R. Weller, "Not so quiet on the ocean front," *Nature*, vol. 348, pp. 199–200, 1990.

[28] C. N. Flagg and S. L. Smith, "On the use of acoustic Doppler current profiler to measure zooplankton abundance," *Deep-Sea Res.*, vol. 36, pp. 455–474, 1989.

[29] E. S. Johnson, "A convergent instability wave front in the central tropical Pacific.," *Deep-Sea Res.*, vol. 43, pp. 753–778, 1996.

[30] D. G. Foley, T. D. Dickey, R. R. Bidigare, M. Ondrusek, R. T. Barber, S. Lindley, M. J. McPhaden, and C. Trees, "Intra-seasonal variations of primary productivity in the central equatorial Pacific Ocean," *Geophys. Res. Letters*, vol. submitted, 1997.

[31] M. R. Landry, J. Kirshtein, and J. Constantinou, "Abundances and distributions of picoplankton populations in the central equatorial Pacific," *Deep-Sea Res.*, vol. submitted, 1996.

[32] C. R. Smith, D. J. Hoover, S. E. Doan, R. H. Pope, D. J. DeMaster, F. C. Dobbs, and M. A. Altabet, "Phytodetritus at the abyssal seafloor across 10 degrees of latitude in the central equatorial pacific," *Deep-Sea Res.*, vol. submitted, 1996.

[33] M. Sawyer and P. Flament, "A three-dimensional view of the equatorial front," *Deep-Sea Res.*, vol. 42, 1995. cover.